(12)

EDGEWOOD
RESEARCH,
DEVELOPMENT &
ENGINEERING
CENTER

ERDEC-TR-093

SCREENING SMOKE PERFORMANCE OF COMMERCIALLY AVAILABLE POWDERS I. INFRARED SCREENING BY GRAPHITE FLAKE

Janon F. Embury
Donald L. Walker

RESEARCH AND TECHNOLOGY DIRECTORATE

Curtis J. Zimmermann

GEO-CENTERS, INC.
Fort Washington, MD 20744

July 1993

U.S. ARMY
CHEMICAL
AND BIOLOGICAL
DEFENSE AGENCY

Aberdeen Proving Ground, Maryland 21010-5423

Disclaimer

The findings in this report are not to be construed as an official Department of the Army position unless so designated by other authorizing documents.

REPORT DOCUMENTATION PAGE

Form Approved
OMB No. 0704-0188

1. AGENCY USE ONLY (Leave blank)	2. REPORT DATE	3. REPORT TYPE AND DATES COVERED
	1993 July	Final, 91 Aug - 93 Feb

4. TITLE AND SUBTITLE

Screening Smoke Performance of Commercially Available Powders
I. Infrared Screening by Graphite Flake

5. FUNDING NUMBERS

PR-10464609D200

6. AUTHOR(S)

Embury, Janon F.; Walker, Donald L. (ERDEC); and
Zimmermann, Curtis J. (GEO-CENTERS, Inc.)

7. PERFORMING ORGANIZATION NAME(S) AND ADDRESS(ES)

DIR, ERDEC,* ATTN: SCBRD-RTB, APG, MD 21010-5423

GEO-CENTERS, Inc., Fort Washington, MD 20744

8. PERFORMING ORGANIZATION REPORT NUMBER

ERDEC-TR-093

9. SPONSORING/MONITORING AGENCY NAME(S) AND ADDRESS(ES)

10. SPONSORING/MONITORING AGENCY REPORT NUMBER

11. SUPPLEMENTARY NOTES

*When this work was performed, ERDEC was known as the U.S. Army Chemical Research, Development and Engineering Center, and the ERDEC authors were assigned to the Research Directorate.

12a. DISTRIBUTION/AVAILABILITY STATEMENT

Approved for public release; distribution is unlimited.

12b. DISTRIBUTION CODE

13. ABSTRACT (Maximum 200 words)

Commercially available graphite powders are evaluated in the U.S. Army Edgewood Research, Development and Engineering Center Smoke Chamber. Figures of merit for weight, volume, and cost constrained applications are described to rate the screening ability of these materials in the visible and infrared. Fundamental properties called "performance parameters" are identified (extinction coefficient, deposition velocity, packing density, and dissemination yield) for measurements so that chamber characterization can be used to predict smoke performance in the battlefield.

14. SUBJECT TERMS

Smoke materials; Infrared screening; Obscurants; IR extinction; IR absorption; Powder technology

15. NUMBER OF PAGES

31

16. PRICE CODE

17. SECURITY CLASSIFICATION OF REPORT	18. SECURITY CLASSIFICATION OF THIS PAGE	19. SECURITY CLASSIFICATION OF ABSTRACT	20. LIMITATION OF ABSTRACT
UNCLASSIFIED	UNCLASSIFIED	UNCLASSIFIED	UL

Blank

PREFACE

The work described in this report was authorized under Project No. 10464609D200, Screening Smoke Material Engineering. This work was started in August 1991 and completed in February 1993.

The use of trade names or manufacturers' names in this report does not constitute an official endorsement of any commercial products. This report may not be cited for purposes of advertisement.

This report has been approved for release to the public. Registered users should request additional copies from the Defense Technical Information Center; unregistered users should direct such requests to the National Technical Information Service.

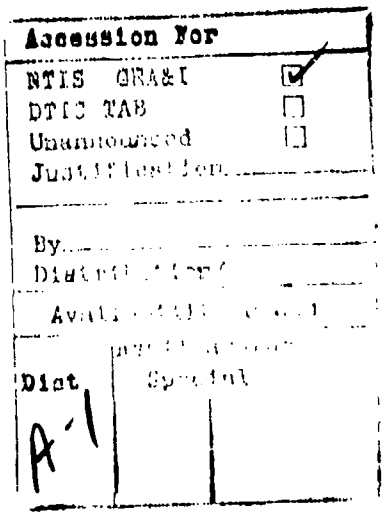

Blank

CONTENTS

LIST OF FIGURES AND TABLES

Figure

Table

SCREENING SMOKE PERFORMANCE OF COMMERCIALLY AVAILABLE POWDERS I. INFRARED SCREENING BY GRAPHITE FLAKE

INTRODUCTION

To measure a material's ability to screen in selected regions of the electromagnetic spectrum it is necessary to characterize the smoke material in terms of its performance parameters and figures of merit. The ratio of aerosol mass to transported precursor material mass is called "yield factor", or simply "yield" (Y) and is the first performance parameter that is used to judge smoke screening performance of a material. The second performance parameter that measures smoke screening performance is the electromagnetic extinction cross section per mass of aerosol and is generally represented by and referred to as the greek letter alpha, α. It quantifies the size of the "shadow" per mass of material when deployed as a tenuous cloud where no particle is in the shadow of another particle. In other words it is the size of the shadow cast by a single particle divided by the particle mass. The third performance parameter, deposition velocity (υ_D), indicates the rate of aerosol fallout onto the ground as a smoke plume is transported downwind. It can be related to downwind smoke screening performance and takes into account reaerosolization, impaction, sedimentation, and Brownian motion deposition of the smoke material. These three performance parameters have been measured in the ERDEC smoke chamber (Figure 2) and are presented in Table 1. The yield (Y) values correspond to dissemination efficiency of dry powders pneumatically disseminated by the Stanford Research Institute (SRI) sonic velocity nozzle operated at 60 psi.

Phosphorous has been a popular smoke screening material for a long time because it reacts with water vapor and oxygen in the air to produce an optically dense aerosol mass more than three times greater than the starting material mass (yields greater than three). The reaction with air allows the formation of aerosol droplets with a mass median diameter near the optimal value of 3/4 micron (μ) for maximum alpha for visible screening at refractive indices in the range of 1.33-1.5. Phosphorus has an acceptably large alpha in the visible spectral region but not at the longer infrared wavelengths, where smoke screening is required in the atmospheric infrared windows of 3-5 and 8-14 microns (μ) wavelength. Infrared screening is necessary in these regions in order to defeat detectors such as indium-antimonide and mercury-cadmium-telluride that are part of thermal imaging systems working in these respective wavelength bands[1]. Acceptable values for alpha (α) in the infrared are achievable not by using micron size dielectric spherical particles such as those present in phosphorus smoke, but instead by using conductive particles that are either flakes, fibers, foam or bubbles where maximum dimensions are several microns and minimum dimensions (wall thickness in the case of foams and bubbles) become less than about a tenth of a micron. It is very difficult to generate such particles with an in situ chemical reaction pulling mass from the air to contribute to aerosol mass, so the maximum possible dissemination yield is unity.

Text continues on page 15.

PERFORMANCE PARAMETERS AND FIGURES OF MERIT
FOR GRAPHITE SCREENING MATERIALS
CHAMBER TESTS UTILIZING SRI NOZZLE AT 60 PSI

TABLE 1

MATERIAL AND COST[a]	BET SURFACE AREA (m^2/g) PURITY (% C)	PARTICLE DENSITY $\rho(g_d/cm^3)$	YIELD $Y(g_d/g_c)$	DEPOSITION VELOCITY (cm/sec)	AVG ALPHA $\alpha(m^2/g_d)$ 0.45-0.65μm 1.06μm 3.0-5.0μm 8.0-14.0μm	AVG ALPHA*RHO $\alpha*\rho$ (m^2/cm^3)	WEIGHT LIMITED FIGURE OF MERIT $\Phi_W=\alpha*Y$ (m^2/g_d)	VOLUME LIMITED FIGURE OF MERIT $\Phi_V=\alpha*Y*\rho$ (m^2/cm^3)	FINANCIAL LIMITED FIGURE OF MERIT $\Phi_F=\alpha*Y/COST$ ($m^2/\$$)[†]
ASBURY A-98 SYNTHETIC @ $0.70/lb ~50,000 lb	11-15 99.6% C	2.23	0.665	0.365	0.82 0.90 0.94 0.95	1.83 2.01 2.10 2.12	0.55 0.60 0.62 0.63	1.22 1.33 1.40 1.41	356.7 389.1 402.1 408.6
ASBURY MICRO 150 NATURAL @ $1.20/lb ~50,000 lb	22-25 82.4% C	2.28	0.930	0.101	2.69 2.65 2.19 1.1	6.13 6.04 4.99 2.51	2.50 2.46 2.04 1.02	5.70 5.62 4.64 2.33	945.8 930.7 771.8 385.9
ASBURY MICRO 250 SYNTHETIC @ $1.90/lb ~50,000 lb	18-20 99.9% C	2.27	0.956	0.131	1.64 1.68 1.78 1.61	3.72 3.81 4.04 3.65	1.57 1.61 1.70 1.54	3.56 3.65 3.86 3.50	375.2 384.7 406.2 367.9

[a] 1C 6.54.23/3.10.28

∞

ASBURY MICRO 260 SYNTHETIC @ $1.90/lb -50,000 lb	17-20 99.9% C	2.27	0.912	0.120	1.70 1.71 1.84 1.65	3.86 3.86 4.18 3.75	1.56 1.56 1.68 1.50	3.52 3.54 3.81 3.41	372.7 372.7 401.4 358.4
ASBURY ULTRA FINE 440 SYNTHETIC @ $4.10/lb -50,000 lb	-84.7 99.5% C	2.27	0.491	0.325	0.79 0.81 0.88 0.88	1.79 1.84 2.00 2.00	0.39 0.40 0.43 0.43	0.88 0.90 0.98 0.98	43.2 44.3 47.6 47.6
ASBURY MICRO 450 SYNTHETIC @ $1.45/lb -50,000 lb	25-30 99.1% C	2.27	0.966	0.068	1.91 1.94 2.07 1.79	4.34 4.40 4.70 4.06	1.85 1.87 2.00 1.73	4.19 4.25 4.54 3.93	579.2 585.5 626.2 541.7
ASBURY MICRO 460 SYNTHETIC @ $1.45/lb -50,000	22-26 99.5% C	2.27	0.956	0.090	1.85 1.88 2.01 1.76	4.20 4.27 4.56 4.00	1.77 1.80 1.92 1.68	4.01 4.08 4.36 3.82	554.2 563.6 601.2 526.0
ASBURY 508 NATURAL @ $0.35/lb -50,000 lb	18-20 83.2% C	2.28	0.781	0.361	1.06 1.05 0.96 0.70	2.42 2.39 2.19 1.60	0.83 0.82 0.75 0.54	1.89 1.87 1.71 1.25	1,070.5 1,057.6 967.3 696.5
ASBURY MICRO 750 NATURAL @ $1.65/lb -50,000 lb	10-15 96.5% C	2.29	0.960	0.087	2.00 2.03 2.18 1.72	4.58 4.65 4.99 3.94	1.92 1.95 2.09 1.65	4.40 4.46 4.80 3.78	528.3 536.5 575.1 454.0
ASBURY 999 NATURAL @ $0.58/lb -50,000 lb	 83.3% C	2.28	0.926	0.131	2.17 2.15 1.88 1.06	4.95 4.90 4.29 2.42	2.01 1.99 1.74 0.98	4.58 4.54 3.97 2.24	1,573.3 1,557.7 1,362.0 767.1

ASBURY 3203 NATURAL @ $0.96/lb ~50,000 lb	10-15 96.3% C	2.29	0.921	0.166	1.39 1.44 1.52 1.46	3.18 3.30 3.48 3.34	1.28 1.33 1.40 1.34	2.93 3.04 3.21 3.08	605.3 628.9 662.1 633.7
ASBURY 3204 NATURAL @ $0.75/lb ~50,000 lb	8-14 96.4% C	2.29	0.858	0.327	0.72 0.82 0.85 0.91	1.65 1.88 1.95 2.08	0.62 0.70 0.73 0.78	1.41 1.61 1.67 1.79	375.3 423.7 441.9 472.2
ASBURY 3442 NATURAL @ $2.80/lb ~50,000 lb	12-18 96.8% C	2.29	0.967	0.097	1.77 1.80 1.93 1.76	4.05 4.12 4.42 4.03	1.71 1.74 1.87 1.70	3.92 3.99 4.27 3.90	277.3 282.1 303.2 275.6
ASBURY 7101 NATURAL @ $1.12/lb ~50,000 lb	7-11 99.8	2.23	0.552	0.457	0.72 0.77 0.81 0.80	1.61 1.72 1.81 1.78	0.40 0.43 0.45 0.44	0.89 0.95 1.00 0.98	162.1 174.3 182.4 178.4
CIBA-GEIGY 6154 SYNTHETIC @ $12.15/lb ~50,000 lb	~13.3 99.9% C	2.30	0.891	0.145	1.74 1.80 1.81 1.78	4.00 4.14 4.16 4.09	1.55 1.60 1.61 1.58	3.56 3.69 3.71 3.65	57.9 59.9 60.3 59.3
CIBA-GEIGY 7525 SYNTHETIC @ $8.75/lb ~50,000 lb	~21.0 99.9% C	2.30	0.952	0.058	2.11 2.14 2.30 2.14	4.85 4.92 5.29 4.92	2.01 2.04 2.19 2.04	4.62 4.69 5.04 4.69	104.2 105.7 113.6 105.7
DIXON HPN-2 NATURAL @ $2.53/lb ~44,000 lb	 99.5% C	2.27	0.929	0.083	1.95 1.93 2.09 1.95	4.43 4.38 4.74 4.43	1.81 1.79 1.94 1.81	4.11 4.07 4.41 4.11	325.1 321.2 348.1 324.8

DIXON HPS-2 SYNTHETIC @ $3.05/lb ~44,000 lb	99.9% C	2.27	0.929	0.071	2.04 2.07 2.20 2.09	4.63 4.70 4.99 4.74	1.90 1.92 2.04 1.94	4.30 4.37 4.64 4.41	282.8 285.8 303.6 288.8
DIXON 192-1 @ $15.00/lb ~44,000		2.27	0.765	0.210	2.10 2.03 1.80 1.06	4.77 4.61 4.09 2.41	1.61 1.55 1.38 0.81	3.65 3.53 3.12 1.84	48.7 46.9 41.8 24.5
DIXON 200-08 CRYSTALLINE @ $1.73/lb ~44,000 lb	97.0% C	2.27	0.775	0.229	1.26 1.27 1.33 1.43	2.86 2.88 3.02 3.25	0.98 0.98 1.03 1.10	2.22 2.23 2.34 2.52	257.2 257.2 270.3 288.7
DIXON 200-09 CRYSTALLINE @ $1.83/lb ~44,000 lb	97.0% C	2.27	0.947	0.130	1.39 1.44 1.50 1.56	3.16 3.27 3.41 3.54	1.32 1.36 1.42 1.48	2.99 3.09 3.22 3.35	327.5 337.4 352.3 367.2
DIXON 200-10 NATURAL @ $2.28/lb ~44,000 lb	97.9% C	2.27	0.944	0.135	1.34 1.41 1.47 1.55	3.04 3.20 3.34 3.52	1.27 1.33 1.39 1.46	2.87 3.02 3.15 3.32	252.9 264.8 276.8 290.7
DIXON 200-39 SYNTHETIC @ $2.89/lb ~44,000 lb	99.4% C	2.27	0.948	0.110	1.75 1.78 1.90 1.81	3.97 4.04 4.31 4.11	1.66 1.69 1.80 1.72	3.77 3.83 4.09 3.89	260.8 265.5 282.8 270.2
DIXON 200-42 SYNTHETIC @ $1.35/lb ~44,000 lb	99.1% C	2.27	0.930	0.150	1.42 1.46 1.54 1.54	3.22 3.31 3.50 3.50	1.32 1.36 1.43 1.43	3.00 3.08 3.25 3.25	443.9 457.4 480.9 480.9

DIXON 200-44 FLAKE @ $1.02/lb ~44,000 lb	96.0% C	2.27	0.938	0.168	1.28 1.32 1.36 1.42	2.91 3.00 3.09 3.22	1.20 1.24 1.28 1.33	2.72 2.81 2.90 3.02	534.1 551.9 569.7 591.9
LONZA E-KS-4 SYNTHETIC @ $5.25/lb	~24.7 99.9% C	2.25	0.944	0.056	2.35 2.36 2.55 2.06	5.29 5.31 5.74 4.64	2.22 2.23 2.41 1.94	4.99 5.01 5.42 4.38	191.8 192.6 208.2 168.2
LONZA KS-6 SYNTHETIC @ $3.00/lb ~28,400 lb	~20 99.9% C	2.26	0.961	0.064	2.24 2.27 2.43 2.22	5.06 5.13 5.49 5.02	2.15 2.18 2.34 2.13	4.87 4.93 5.28 4.82	325.8 330.1 353.4 322.9
LONZA SFG-6 SYNTHETIC @ $3.54/lb ~28,400 lb	~20 99.9% C	2.26	0.968	0.050	2.29 2.33 2.45 2.31	5.18 5.27 5.54 5.22	2.22 2.26 2.37 2.24	5.01 5.10 5.36 5.05	284.3 289.2 304.2 286.8
LONZA KS-10 SYNTHETIC @ $2.20/lb ~28,400	~18 99.9% C	2.25	0.941	0.107	1.39 1.45 1.52 1.55	3.13 3.26 3.42 3.49	1.31 1.36 1.43 1.46	2.94 3.07 3.22 3.28	269.9 281.6 295.2 300.9
LONZA SFG-10 SYNTHETIC @ $2.91/lb ~28,400	~11 99.9% C	2.24	0.963	0.102	1.41 1.49 1.56 1.64	3.16 3.34 3.49 3.67	1.36 1.44 1.50 1.58	3.04 3.21 3.37 3.54	211.8 223.8 234.4 246.4
LONZA KS-15 SYNTHETIC @ $1.93/lb ~37,000 lb	~14 99.9% C	2.24	0.928	0.164	1.19 1.25 1.30 1.36	2.67 2.80 2.91 3.05	1.10 1.16 1.21 1.26	2.47 2.60 2.70 2.83	259.8 272.9 283.8 296.9

LONZA T-15 SYNTHETIC @ $1.98/lb ~37,850 lb	~15 99.9% C	2.24	0.955	0.142	1.21 1.29 1.33 1.35	2.71 2.89 2.98 3.02	1.16 1.23 1.27 1.29	2.59 2.76 2.84 2.89	264.9 282.5 291.2 295.6
SUPERIOR 2939 @ $1.30/lb ~20 Tons	~12.5 99.8% C	2.21	0.912	0.155	1.56 1.62 1.67 1.55	3.45 3.58 3.69 3.43	1.42 1.48 1.52 1.41	3.14 3.26 3.37 3.12	495.9 516.9 530.8 492.4
SUPERIOR 3739 @ $0.71/lb ~20 Tons	~28.9 78.0% C	2.22	0.918	0.161	1.68 1.68 1.56 1.10	3.73 3.73 3.46 2.44	1.54 1.54 1.43 1.01	3.42 3.42 3.18 2.24	984.7 984.7 914.4 645.8
SUPERIOR 3839 @ $0.78/lb ~20 Tons	~25.0 85.0% C	2.22	0.908	0.158	1.69 1.68 1.56 1.09	3.75 3.73 3.46 2.42	1.54 1.53 1.42 0.99	3.41 3.39 3.15 2.20	896.4 890.5 826.5 576.2
SUPERIOR 4739 CRYSTALLINE VEIN @ $ 2.17/lb ~20 Tons	~8.50 98.6% C	2.20	0.889	0.294	0.85 0.89 0.93 0.97	2.16 1.96 2.05 2.13	0.76 0.79 0.83 0.86	1.66 1.74 1.82 1.90	158.1 165.5 172.9 180.4
SUPERIOR 4939 CRYSTALLINE VEIN @ $2.62/lb ~20 Tons	~12.5 99.8% C	2.20	0.911	0.218	0.98 1.05 1.10 1.12	2.16 2.31 2.42 2.46	0.89 0.96 1.00 1.02	1.96 2.10 2.20 2.24	154.2 166.4 173.3 176.7
SUPERIOR 5039 SYNTHETIC @ $1.19/lb ~20 Tons	~14.70 99.0% C	2.20	0.913	0.199	1.35 1.26 1.31 1.23	2.97 2.77 2.88 2.71	1.23 1.15 1.20 1.12	2.71 2.53 2.63 2.47	469.3 438.7 457.8 427.3

SUPERIOR 5539 SYNTHETIC @ $1.64/lb ~20 Tons	10-15 99.8% C	2.15	0.839	0.235	1.02 1.07 1.14 1.16	2.19 2.30 2.45 2.49	0.86 0.90 0.96 0.97	1.84 1.93 2.06 2.09	238.1 249.2 265.8 268.5
SUPERIOR 8539 CRYSTALLINE FLAKE @ $1.55/lb ~20 Tons	~10.79 98.0% C	2.20	0.888	0.254	0.97 1.02 1.07 1.10	2.13 2.24 2.35 2.42	0.86 0.91 0.95 0.98	1.90 2.00 2.09 2.15	251.9 266.5 278.3 287.1
SUPERIOR 9039 DESULCO @ $0.80/lb ~20 Tons	~17.7 99.5% C	2.20	0.889	0.232	1.09 1.14 1.20 1.13	2.40 2.51 2.64 2.49	0.97 1.01 1.07 1.00	2.13 2.23 2.35 2.21	550.5 573.2 607.2 567.5
SUPERIOR SF-39 SYNTHETIC FLAKE @ $0.62/lb ~20 Tons	~15.0 98.0% C	2.20	0.886	0.271	0.94 1.00 1.04 1.05	2.07 2.20 2.29 2.31	0.83 0.89 0.92 0.93	1.83 1.95 2.03 2.05	607.7 651.7 673.7 681.0

AVERAGE ALPHA VALUES SELECTED FOR FOLLOWING REASONS:

0.45-0.65μm visible light corresponds to the range of maximum photopic and scotopic response for the human eye.

1.06μm is the operating wavelength of neodinium YAG laser designators.

3.0-5.0μm is the operating regime for thermal imaging systems that rely on indium antimonide detectors.

8.0-14.0μm is the operating regime for thermal imaging systems that rely on mercury cadmium telluride detectors.

g_a=grams aerosol, g_d=grams disseminated=grams transported

†($/lb)(lb/454$g_a$)

§ cost of graphite materials is an approximation given by the individual suppliers and may not reflect the actual cost.

EXTINCTION COEFFICIENTS OF CONDUCTIVE FLAKES, FOAM PARTICLES AND BUBBLES

Simple theoretical treatments of the electromagnetic extinction cross section per mass, α, of conductive flake, fiber, foam or hollow spheres are possible because of the absence of resonance structure. Orientation distribution, size distribution and absorption due to conductivity all act to remove resonance structure that is so apparent in the cross section spectra of monodisperse nonabsorbing dielectric spheres. For conductive flake, foam and hollow spheres at wavelengths less than about three times the major particle dimension and for minimum dimensions greater than the skin depth, α lies on a high plateau independent of conductivity and complex refractive index. At longer wavelengths greater than about three times the particles major dimension α decreases below the plateau level eventually with a reciprocal wavelength squared dependence when the absorption cross section dominates and conductivity is represented by the dispersion relation of a free electron metal. One can see an example of this plateau/particle size effect in Figure 1 and Table 1 when comparing the α of Asbury 260 and Lonza E-KS-4 in the near, mid and far infrared regions. The higher α curve is due to a smaller flake major dimension particle size (mass median diameter) and a thinner flake thickness (minor dimension).

For best screening performance in the near, mid and far infrared spectrum we want particles that lie on this high plateau with major dimensions greater or equal to about four microns that extend the plateau across the atmospheric infrared windows out approaching 14 microns wavelength. The level of the plateau will now be shown to be inversely proportional to flake thickness and foam or bubble wall thickness using the geometric optics theory to explain extinction of radiation by polydispersions of randomly orientated absorbing flakes, foams and bubbles throughout the plateau. Here the efficiency factor (Q) for extinction, the ratio of electromagnetic extinction cross section divided by geometric cross section,is approximately equal to two ($Q \approx 2$), an approximation that becomes more accurate at wavelengths much smaller than particle dimensions.

At wavelengths on the order of particle dimensions the efficiency factor represents an average over the largest resonances that appear in single particle cross section spectra so Q is somewhat higher especially when averaged over the lowest order resonant modes closest to the plateau edge. However, as apparent from continuous cross section spectral scans such as Figure 1 the peak value for α is broad and no more than about 20% greater than the value for α at shorter wavelengths. Thus the theory of geometric optics serves as a reasonable approximation, beyond the typical region where all particle dimensions are much greater than the radiation wavelength, on through the resonance region where resonance structure is washed out by size and orientation distribution yielding Q and α values only slightly greater than at the shorter wavelengths where the geometric optics theory is more strictly valid. At longer wavelengths beyond the plateau α drops quickly with increasing wavelength and the geometric optics treatment is no longer applicable.

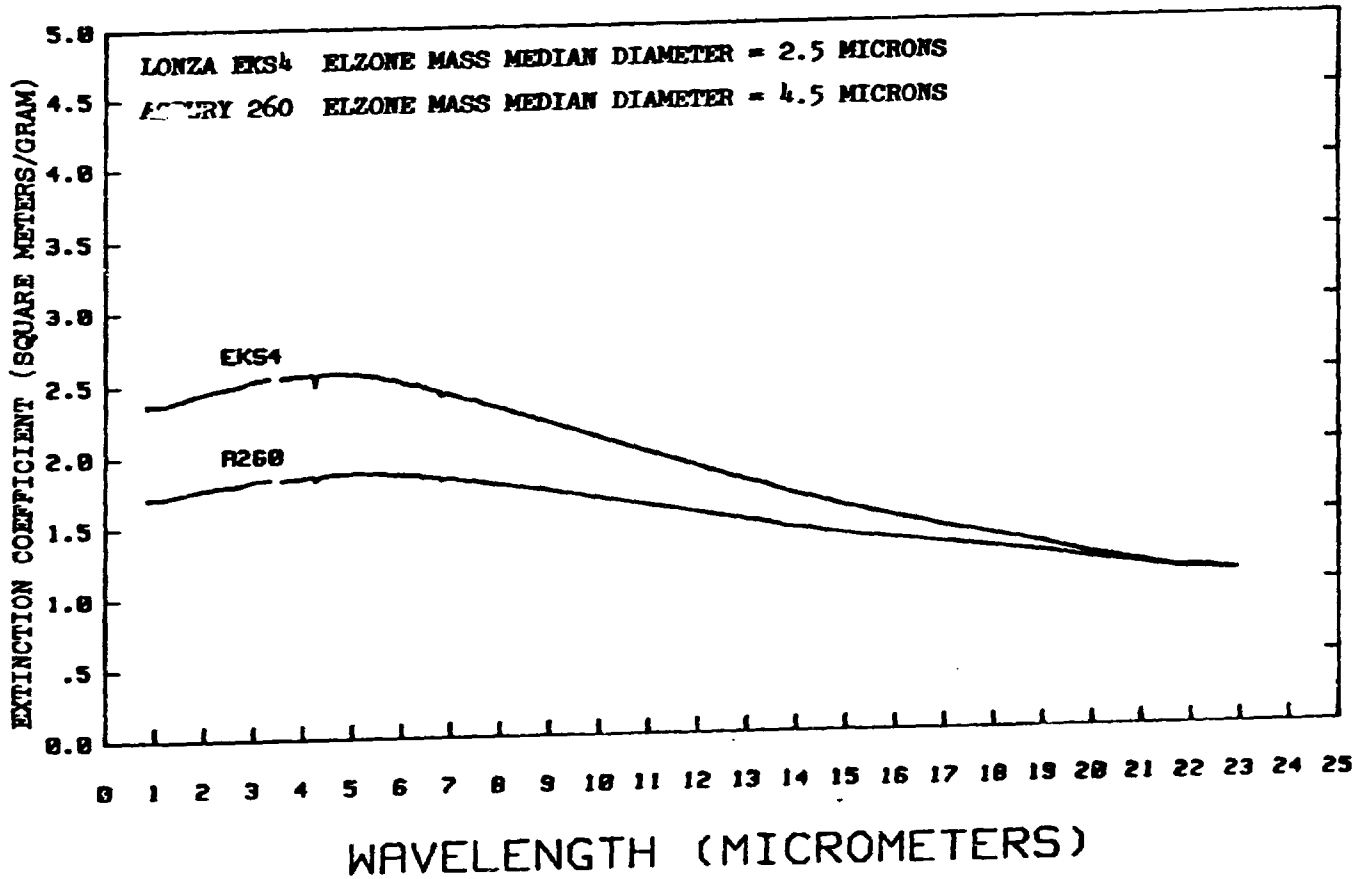

Figure 1. Infrared Extinction Spectra of Asbury 260 and Lonza EKS4

Combine the earlier definition of Q, the ratio of the electromagnetic extinction cross section divided by the geometric cross section G, with the definition of α, the electromagnetic extinction cross section per mass ρV of material where ρ is the particle density and V is the particle volume, averaged over random orientation angles[2]Ω

$$\langle \alpha \rangle_\Omega = \left\langle \frac{QG}{\rho V} \right\rangle_\Omega = \frac{\langle QG \rangle_\Omega}{\rho V}$$

If we assume major particle dimensions are greater than about one third of the wavelength, then the geometric optics solution puts Q=2 and if we assume particles are randomly orientated and convex, a well known result puts the geometric cross section $\langle G \rangle_\Omega = S/4$ equal to one fourth the surface area. Thus we find that α averaged over random orientation becomes

$$\langle \alpha \rangle_\Omega = \frac{2\,S/4}{\rho V} = \frac{S}{2\rho V}$$

For our flake particles $S/V = 2/t_w$ where t_w is the flake thickness. For bubbles and spherical foam particles of radius R we have $S/V = 3/R$ at a reduced density ρ' which becomes in the case of a bubble with wall thickness t_w

$$\rho' = \frac{4\pi R^2 t_w}{\frac{4}{3}\pi R^3}\rho = \frac{3\,t_w}{R}\rho$$

A foam particle of radius R may be considered to consist of a large number N of roughly spherical cells having radius r and cell wall thickness t_w. Because adjacent cells share walls, total foam particle mass may be expressed as the sum of the masses of N bubbles having radius r and wall thickness $t_w/2$ plus a single envelope bubble of radius R and wall thickness $t_w/2$. Noting that $N = R^3/r^3$ we find a reduced density ρ' for the foam particle

$$\rho' = \frac{3\,t_w}{2}\left(\frac{1}{r} + \frac{1}{R}\right)\rho$$

Thus the extinction coefficients comparing these three types of particles averaged over random orientations become

$$\langle\alpha\rangle_a = \begin{cases} \dfrac{1}{\rho t_w} & \text{for flakes} \\ \dfrac{1}{2\rho t_w} & \text{for bubbles} \\ \dfrac{1}{\left(\dfrac{R}{r}+1\right)\rho t_w} & \text{for foams} \end{cases}$$

A convenient and self consistent set of units puts particle dimensions in microns, density ρ in g/cm^3 and α in m^2/g. We need conductive (even very strongly absorbing dielectrics are not sufficiently broadband) flakes, foam particles or bubbles with major dimension greater than one third the maximum wavelength to be screened with the smallest possible minimum dimension in order to maximize α throughout the spectral region.

GRAPHITE FLAKE MANUFACTURING

Unless the conductive foam and bubble aerosol particles are produced in the field, from a liquid for example, they have to be transported as foam and hollow spheres with solid walls at prohibitively low packing densities. Conductive fibers longer than several microns with diameters on the order of and less than a tenth of a micron are available commercially as graphite from Hyperion and experimental quantities of iron whiskers with this morphology have been made by 3M. Graphite fiber is not desirable from a toxicological point of view because it does not break up in the lungs and the morphology is similar to that of asbestos. It has been shown that explosive dissemination of carbon fibers results in the presence of fiber fragments and combustion products in the respirable range[3]. Conductive flakes are available commercially and graphite flakes have distinct advantages over the earlier infrared screeners, brass and aluminum flakes[4]. Graphite flakes are not toxic to aquatic life in the environment, in contrast to brass flakes, and graphite flake aerosol does not suffer a flashing problem near a dissemination source as aluminum flake does because of its reactivity. Furthermore, as a refractory material graphite will not undergo cold welding during explosive dissemination. Thus among the various types of conductive particles that screen effectively in the infrared, only graphite flake is acceptable on all counts.

Graphite flake falls into two categories; natural (mined) and synthetic. Carbon having the true graphitic structure is available commercially from naturally occurring feedstock (embedded in minerals) and synthetic fabrication. Natural graphite is known to occur in three different forms, each produced from different geological conditions.

Natural flake graphite is found in metamorphose rocks that have undergone plastic flow. Vein graphite, also known as lump graphite, is found as veins throughout rock structures. This material being deposited as a result of decomposed carbon-rich materials that later transformed to graphite under pyrogenic conditions. The third distinct form is amorphous graphite which results from graphitization of coal deposits due to the presence of molten magma. These different forms of graphite are rarely found together due to their different geological origins. Synthetic graphite is produced typically from petroleum coke (a byproduct of the petroleum cracking process) or anthracite coal calcined to high temperatures (electrothermal graphitization). Conversion of the feed stock to produce synthetic graphite may have a yield as high as 85%. Identification of synthetic graphite is rather simple since it will have a carbon content of at least 99% and the residual ash after ignition will contain silicon carbide[5]. The resulting produced graphitic solid is then coarse ground and finally processed via ball and/or jet milling to yield a fine "flake" like powder. Stringent control over particle size reduction leads to uniformly sized powders. Air classification can be utilized to provide the milled powders in a particular particle size and narrow size distribution. The calculated density for graphite is ~2.26g/cm^3 and has a Mohs scale of hardness of ~0.5-1.5 depending on the different structures[5,6]. It is important to remember that only naturally occurring flake graphite represents a true flake (analogous to mica) and is capable of being intercalated and exfoliated to yield very thin flakes having high aspect ratios[7]. Synthetic graphite's "flake" like morphology is a result of many factors including the petroleum fraction calcined, orientation of the crystallites and the nature of the milling operations. Natural graphite can be mined as both crystalline flake and vein graphite, with the flake more true in shape being analogous to mica. The natural graphites are known to contain a small amount of silica as a contaminant, the concentration of which depends on the geological origin of the graphite. A small fraction of this silica may be in the crystalline form, which must be restricted to very low levels under 1/2% because of inhalation toxicity. It would be of great interest to determine the ratio of crystalline to amorphous silica present in a natural graphite material and determine via inhalation studies if there exists an inhalation toxicity associated with natural graphite flake. Because of the morphology differences between natural and synthetic graphite, further processing of the commercial flake including ball and/or jet milling, air classification, powder densification and grinding for deagglomeration could prove more advantageous to one graphite form than the other[8].

ERDEC SMOKE CHAMBER AND DATA COMPUTATIONAL ALGORITHMS

The 14 cubic meter smoke chamber used to measure the performance parameters such as the electromagnetic extinction cross section per mass of aerosol (α), yield (Y) and deposition velocity (υ_D) is shown in Figure 2 with the full smoke characterization instrument configuration. Glass fiber filters, a rotometer and vacuum pump are used to make aerosol concentration measurements at a flow rate of 20 liters per minute. A photodiode array spectrometer measures aerosol transmittance over the wavelength range of 0.4μ-1.0μ. Two FTIR spectrometers measure aerosol transmittance over the spectral regions 0.9μ-3μ and 2.5μ-22μ. At reduced concentrations a quartz crystal microbalance (QCM) and an aerodynamic particle sizer (APS) measure aerodynamic particle size distribution. The Stanford Research Institute sonic pneumatic nozzle is operated at 60 psi to disperse and deaggregate powders to produce an aerosol of primary particles[9]. A mixing fan is operated continuously in the chamber at a low speed to maintain uniform concentration and provide a level of turbulence driving reaerosolization and impaction approximating those components of aerosol deposition in the battlefield. The aerosol sedimentation component of deposition will of course be independent of whether the aerosol is in a chamber or on the battlefield.

Dissemination yield and deposition velocity are computed based on a series of two filter concentration measurements. Using the stirred settling model[10] to describe the situation where concentration is maintained uniform throughout the chamber by a mixing fan, we find the instantaneous concentration C as a function of time t, initial concentration C_o, deposition velocity υ_D and chamber height H

$$C = C_0 e^{-\upsilon_D t/H}$$

This expression in combination with two filter concentration measurements $C_F(t_1)$ and $C_F(t_2)$ taken over time intervals t_1 to $t_1+\tau$ and t_2 to $t_2+\tau$ respectively allows computation of C_o and υ_D as follows. The filter concentration measurement accumulates incremental mass dm contained in incremental volume dV over time t through $t+\tau$. Because the air pump flow rate through the filter is monitored with a rotometer and held constant at dV/dt we have

$$C_F = \frac{\int dm}{\int dV} = \frac{\int \frac{dm}{dV}\frac{dV}{dt}dt}{\int \frac{dV}{dt}dt} = \frac{\frac{dV}{dt}\int \frac{dm}{dV}dt}{\frac{dV}{dt}\int dt} = \frac{\int \frac{dm}{dV}dt}{\int dt}$$

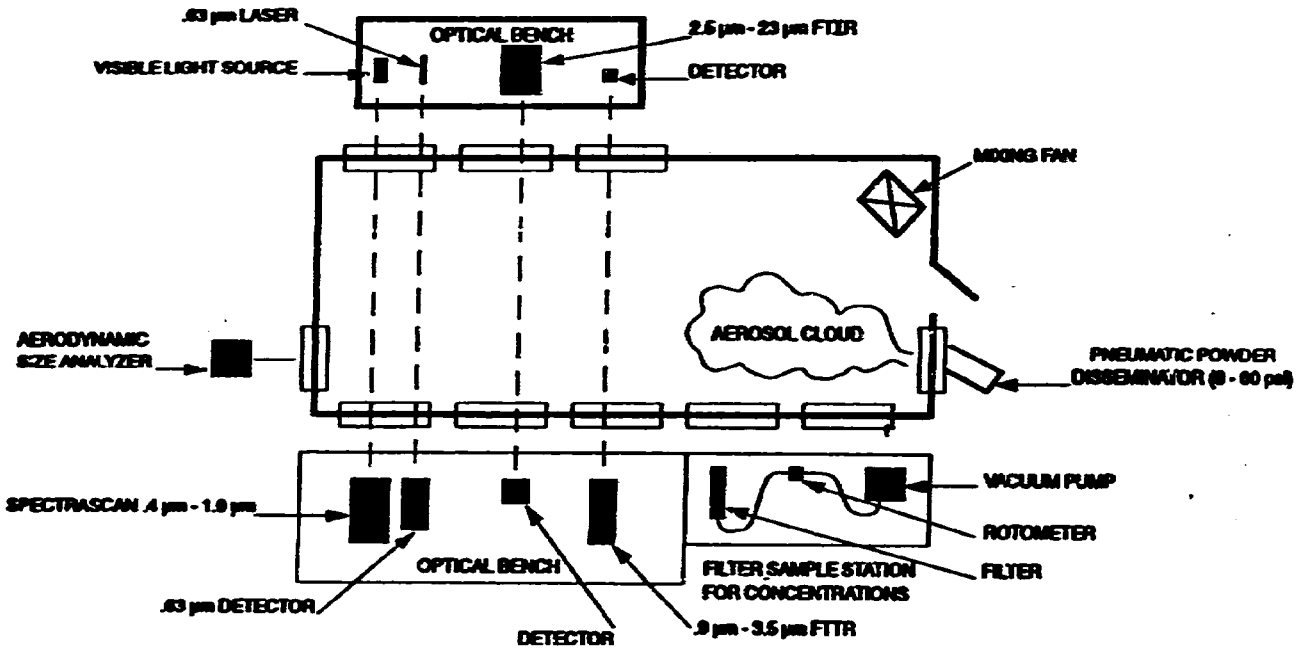

Figure 2. 13.6 M^3 Aerosol Characterization Facility

We identify dm/dV as the instantaneous concentration C so substituting the stirred settling expression

$$C_F = \frac{\int_t^{t+\tau} C_0 e^{-\upsilon_D t/H}\, dt}{\int_t^{t+\tau} dt} = \frac{C_0 H}{\upsilon_D \tau} e^{\frac{-\upsilon_D t}{H}} \left(1 - e^{\frac{-\upsilon_D \tau}{H}}\right)$$

Taking the ratio of the second filter concentration divided by the first, the duration of both measurements being τ

$$\frac{C_F(t_2)}{C_F(t_1)} = e^{-\frac{\upsilon_D}{H}(t_1 - t_2)}$$

so that the third screening smoke performance parameter deposition velocity is

$$\upsilon_D = \frac{H}{t_2 - t_1} \ln \frac{C_F(t_1)}{C_F(t_2)}$$

Solving for the initial concentration

$$C_o = \frac{C_F \upsilon_D \tau}{H} \left(1 - e^{\frac{-\upsilon_D \tau}{H}}\right)^{-1} e^{\frac{\upsilon_D \tau}{H}}$$

the dissemination yield Y is found knowing chamber volume V and measuring mass disseminated m

$$Y = \frac{C_o V}{m}$$

The extinction coefficient is computed using Beers law along with measurements of concentration C and transmittance T with knowledge of transmissometer path length L through the smoke

$$\alpha = \frac{1}{CL} \ln \frac{1}{T}$$

HOMOGENEOUS ELLIPTICAL HALF CONE SMOKE PLUME WITH AEROSOL DEPOSITION

We can judge the performance of a screening smoke material based on the optical depth $\bar{\alpha}CL$ of a smoke plume produced from that material and the duration τ of the plume.

$$\bar{\alpha}CL = \int_{-\infty}^{+\infty} \alpha(l)C(l)dl$$

The integration over variable l is along the line of sight, $\bar{\alpha}$ is the average extinction coefficient along the line of sight, but we should not think of CL as anything more than the areal density of smoke over the line of sight. If the cloud boundaries were defined and L could be specified then $\bar{C}$ could be thought of as concentration C averaged over inhomogeneities along the line of sight, but this is true only in a chamber. This is evident when we define averages

$$\bar{\alpha} = \frac{\int_{-\infty}^{+\infty} \alpha(l)C(l)dl}{\int_{-\infty}^{+\infty} C(l)dl}$$

$$\bar{C} = \frac{\int_{-\infty}^{+\infty} C(l)dl}{\int_{-\infty}^{+\infty} dl}$$

We now develop an expression for smoke areal density CL downwind by using an elliptic half cone smoke plume model in which there is complete mixing. This gives nearly the same result as the Gaussian Plume model incorporating deposition and is simpler to describe.

We approximate the areal density CL of a smoke plume along a horizontal crosswind path and along a vertical crosswind path through the plume centroid path by developing an expression here for a homogeneous plume whose boundaries are defined by an elliptical half cone. The cross sectional area of the elliptical half-cone is $\pi HL/2$ where H is the plume height and L is the width. Mass conservation requires that the decrease in plume incremental mass m as it progresses downwind in direction x satisfy the expression

$$\frac{dm}{dx} = -\frac{d}{dx}(C\frac{\pi}{2}HLdx)$$

The deposition velocity υ_D governs the mass loss over the ground surface area Ldx

$$\frac{dm}{dt} = -v_D CLdx$$

Making the substitution dt=dx/υ_W where υ_W is the wind velocity

$$\frac{dm}{dx} = -\frac{v_D}{v_W}CLdx$$

Setting the above two expressions equal to one another

$$\frac{v_D}{v_W}CL = \frac{d}{dx}(C\frac{\pi}{2}HL)$$

Because the concentration, plume height and width are functions of downwind distance x

$$\frac{v_D}{v_W}CL = \frac{\pi}{2}(HL\frac{dC}{dx} + CL\frac{dH}{dx} + CH\frac{dL}{dx})$$

Using the relationships that have been developed for elliptical half-cone plumes with a Gaussian concentration profile

$$L = a_L x^{b_L}$$

and

$$H = a_H x^{b_H}$$

where the coefficients a_L, a_H, b_L and b_H depend on Pasquill category and terrain roughness. Thus

$$\frac{v_D}{v_W}CL = \frac{\pi}{2}(HL\frac{dC}{dx} + CLa_H b_H x^{b_H-1} + CHa_L b_L x^{b_L-1})$$

Rewriting

$$\frac{dC/dx}{C} = \frac{2}{\pi}\frac{v_D/v_W}{a_H x^{b_H}} - \frac{(b_H+b_L)}{x}$$

Solving in terms of an initial concentration C_o at an arbitrary initial distance x_o downwind close to the generator

$$\ln\frac{C}{C_o}=(b_H+b_L)\ln\frac{x_o}{x}-\frac{\frac{2}{\pi}v_D x^{1-b_H}}{a_H(1-b_H)v_w}$$

$$C=C_o\left(\frac{x_o}{x}\right)^{(b_H+b_L)} e^{\frac{-\frac{2}{\pi}v_D(x^{1-b_H}-x_o^{1-b_H})}{a_H(1-b_H)v_w}}$$

Mass concentration requires at x_o that the mass flowrate into the air, the flowrate out of the generator $\dot{m}$ multiplied by dissemination yield Y, satisfy the following equation where the deposition velocity of aerosolized material has not yet had sufficient time to reduce aerosolized mass because of the proximity to the generator, ie.

$$e^{-\frac{2}{\pi}v_D x_o/(a_H(1-b_H)v_w)}\approx 1$$

so that $\dot{m}Y=v_w C_o H_o L_o$. The quantity v_w represents the wind speed and initial plume height H_o and breadth L_o may be written

$$H_o=a_H x_o^{b_H}$$

$$L_o=a_L x_o^{b_L}$$

Solving for initial concentration

$$C_o=\frac{\dot{m}Y}{\frac{\pi}{2}v_w a_H a_L x_o^{b_H+b_L}}$$

and substituting this into the expression for downwind concentration

$$C=\frac{\dot{m}Y}{\frac{\pi}{2}v_w a_H a_L x^{b_H+b_L}}\, e^{\frac{-\frac{2}{\pi}v_d x^{1-b_H}}{a_H(1-b_H)v_w}}$$

The crosswind horizontal optical depth of the plume near the ground is

$$\alpha CL=\frac{\alpha\dot{m}Y}{\frac{\pi}{2}v_w a_H x^{b_H}}\, e^{\frac{-\frac{2}{\pi}v_d x^{1-b_H}}{a_H(1-b_H)v_w}}$$

and the vertical optical depth at the plume center is

$$\alpha CH=\frac{\alpha\dot{m}Y}{\frac{\pi}{2}v_w a_L x^{b_L}}\, e^{-\frac{2}{\pi}\frac{v_d x^{1-b_H}}{a_H(1-b_H)v_w}}$$

FIGURES OF MERIT

We write the duration of the plume $\tau=M/\dot{m}$ in terms of the average mass flow rate $\dot{m}$ and maximum mass M that can be transported for weight limited applications, while for volume limited applications $\tau=V\rho\dot{m}/$ where V is the maximum volume that can be transported and ρ is the density of smoke material contained in volume V. We can write the crosswind horizontal optical depth

$$\alpha CL=\frac{\alpha\dot{m}Y}{\frac{\pi}{2}Hv_w}\, e^{-\gamma v_d}$$

as a function of wind velocity v_w, dissemination yield Y, plume effective height H, aerosol deposition velocity v_D onto the terrain and a parameter γ that depends on downwind distance, windspeed, Pasquill category and terrain roughness.

$$\gamma=\frac{2\,x^{1-b_H}}{\pi a_H(1-b_H)\,v_w}$$

Defining a goal function $\psi=\alpha CL\tau$ as the product of crosswind optical depth multiplied by duration, we substitute values for duration in weight limited applications such as large area screening

$$\psi_w = \frac{\alpha\dot{m}Y}{\frac{\pi}{2}Hv_w} e^{-\gamma v_o} \frac{M}{\dot{m}} = \frac{M}{\frac{\pi}{2}Hv_w}(\alpha Y e^{-\gamma v_o})$$

and for volume limited applications such as grenades, rockets, smoke pots and mortars

$$\psi_v = \frac{\alpha\dot{m}Y}{\frac{\pi}{2}Hv_w} e^{-\gamma v_o} \frac{V\rho}{\dot{m}} = \frac{V}{\frac{\pi}{2}Hv_w}(\alpha Y\rho e^{-\gamma v_o})$$

The portions of ψ_w and ψ_v that depend on material properties have been put in parentheses and will be called the weight limited Φ_w and volume limited Φ_v figures of merit, respectively. Because we can not remove the dependence of γ upon variables such as windspeed and downwind distance and because within the first few hundred yards downwind $\gamma v_D \approx 0$ is a reasonable approximation for all materials here, we approximate the above two figures of merit as well as a financial limited figure of merit Φ_F that gives the square meters of screening per dollar of cost.

$\Phi_w \approx \alpha Y$ [square meters/gram transported]

$\Phi_v \approx \alpha Y\rho$ [square meters/cubic centimeter transported]

$\Phi_F \approx 454\alpha Y$/cost per pound [square meters/dollar]

These figures of merit depend on the performance parameters α, Y and v_D that we measure in the chamber, packed material density ρ in the storage volume V transported and the cost per pound. An upper limit on ρ is the density of the particle itself and that is the value tabulated. Dimensions of extinction coefficient are screening area per mass of aerosol, yield dimensions are mass of aerosol per mass transported and packing density dimensions are mass transported per volume transported. Thus the dimensions of αY are screening area per mass transported, the dimensions of $\alpha Y\rho$ are screening area per volume transported and the dimensions of the financial figure of merit αY divided by unit cost is square meters of screening per dollar spent.

If a goal function were defined as area screened per mass, volume or cost of material for weight, volume or cost constrained situations, it would be proportional to the same figures of merit for a uniform layer of smoke having depth L and area A. The area screened per mass M, volume V and cost per pound of material \$ are found by requiring that the optical depth produce a transmittance level T_s for effective screening.

$$\alpha YCL = \ln\frac{1}{T_s}$$

This expression provides the value for CL which is then substituted into expressions for area screened per mass, volume and cost to obtain

$$\left(\frac{A}{M}\right)_s = \frac{A}{CAL} = \frac{1}{CL} = \frac{\alpha Y}{\ln\frac{1}{T_s}} = \frac{\Phi_w}{\ln\frac{1}{T_s}}$$

$$\left(\frac{A}{V}\right)_s = \frac{\alpha Y \rho}{\ln\frac{1}{T_s}} = \frac{\Phi_v}{\ln\frac{1}{T_s}}$$

$$\left(\frac{A}{\$}\right)_s = \frac{M}{\$}\frac{\alpha Y}{\ln\frac{1}{T_s}} = \frac{\Phi_r}{\ln\frac{1}{T_s}}$$

Note that for a uniform layer of smoke the area screened per mass, volume or cost of material is just the respective figure of merit when the transmittance required for screening is e^{-1} or equivalently when the required optical depth is unity. Actually the requirement is closer to a transmittance of 5% which corresponds to an optical depth of three in which case the figure of merit should be divided by three to give area screened per mass, volume or cost for a uniform layer of smoke.

BET SURFACE AREA

The approximate BET surface area contained in the first column of Table 1 does not correlate very well with the electromagnetic cross section α. This is evident in Figure 3. No doubt this can be attributed to variability in the porosity (concavity and small pits in the surface) that will increase BET surface area but not α. Using the geometric optics expression developed earlier relating α to envelope surface area S, we can write the approximate relationship

$$\alpha \approx (\text{BET} - \text{Porous Area})/2$$

which shows the effect of porous area. This was explored as a possible alternative to chamber testing with the just mentioned negative result. It is interesting to note that some of the better graphite screening materials have BET surface areas around 25 m^2/g indicating that the porous area dominates over the "envelope" surface area indicated by α.

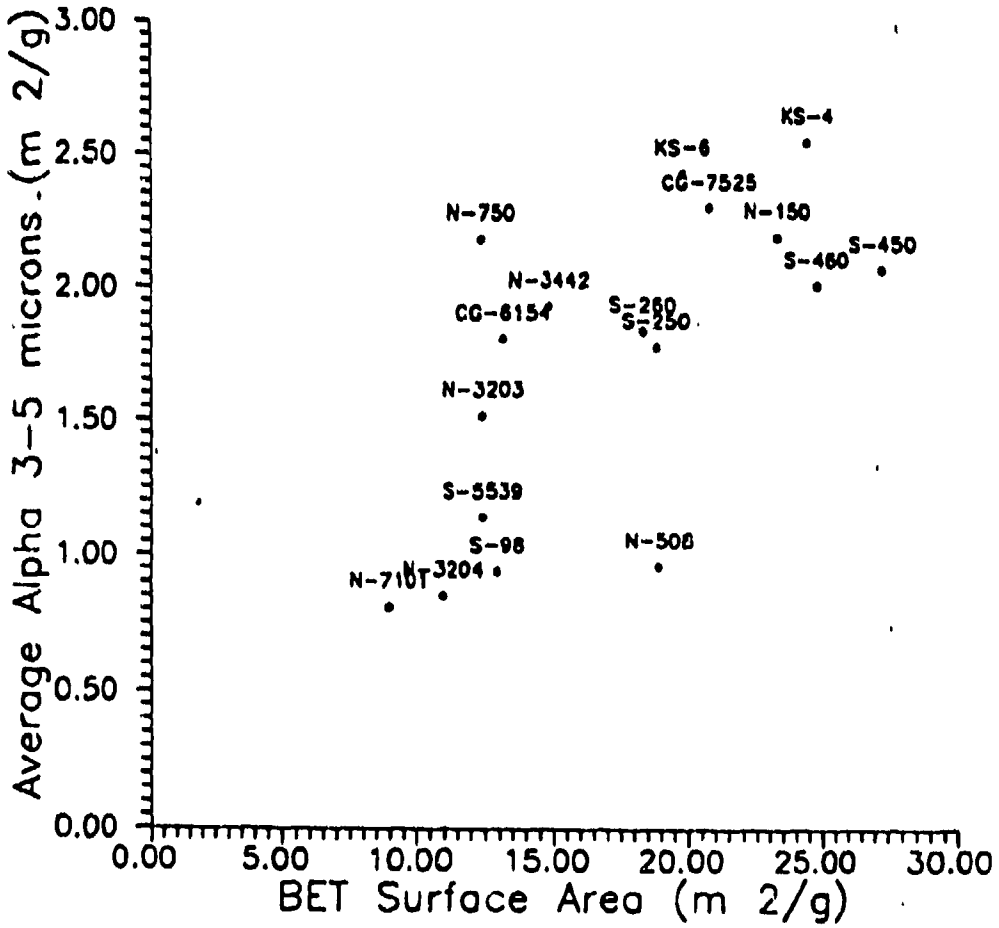

Figure 3. BET Surface Area and Extinction

CONCLUSION

The concept of describing competing smoke materials in terms of four measurable performance parameters (extinction coefficient, dissemination yield, deposition velocity and powder packing density) has been presented. Three figures of merit based on these four performance parameters have been introduced. All three are proportional to smoke plume optical depth downwind and can be used not only to rank performance, but also quantitatively to predict cloud opacities downwind or screening areas. The first figure of merit gives the square meters of smoke screening per mass of smoke material transported and is useful in weight limited applications such as the large area smoke generators. The second figure of merit gives the square meters of screening per volume of smoke material transported and is useful in volume limited applications such as grenades, rockets, artillery rounds, mortars and smoke pots. The third figure of merit gives the square meters of screening per dollar of smoke material cost and is useful in situations such as training with large area smoke screening. Here for example the weight constraint of the large area smoke generator vehicle would have to be met first by specifying a minimum value for the first figure of merit (weight limited) and then comparing all materials satisfying this constraint based on the third figure of merit (financial limited). For example if a minimum weight limited figure of merit (Φ_w) of $1.5m^2/g$ in the 3-5μ region were required so that a sufficient quantity could be transported to accomplish a large area screening mission, the most cost effective material from Table 1 would be Asbury 999 with a financial figure of merit (Φ_F) of $1362m^2/\$$. Toxicity of course might become an issue if the 16.7% non-carbon component is more than 1/2% crystalline quartz.

Graphite flake manufacturing processes were described. Testing of these materials in the ERDEC smoke chamber to obtain dissemination yield, deposition velocity and spectral extinction coefficients from the visible through 20 microns wavelength was also described. Chamber data processing algorithms and downwind homogeneous plume transport including deposition were derived. A wide variety of commercially available graphite powders have been tested in the ERDEC smoke chamber using the SRI sonic pneumatic nozzle at a pressure of 60 psi for dissemination. Performance parameters and their product derived figures of merit are tabulated in Table 1 so that materials can be compared over the visible, 1.06μ, 3-5μ and 8-14μ spectral regions.

LITERATURE CITED

1. Wolfe, W.L. and Zissis, G.J., ed., The Infrared Handbook, The Infrared Information and Analysis (IRIA) Center, Environmental Research Institute of Michigan (1978).
2. Embury, J., "Extinction by Clouds Consisting of Polydisperse and Randomly Orientated Nonspherical Particles at Arbitrary Wavelengths", Optical Engineering, 22(1), 71-77(1983)
3. Smoke/Obscurant Symposium XVI, April 14-16, 71(1992).
4. Shaffer, R., US Patent, 4,484,195(1984).
5. Seeley, S.B., "Natural Graphite," in Encyclopedia of Chemical Technology, Vol. 4, 2nd ed., Wiley-Interscience, New York, 305-355(1964).
6. Hosokawa Micron International, Inc.,"Alpine Handbook of Mechanical Processing Technology",780 Third Avenue, Suite 3201 New York, NY 10017.
7. Kuga, Y., Endoh, S., Chiyoda, H. and Takeuchi, K., Powder Technology, 66,85-88(1991).
8. Embury, J., Walker, D. and Zimmermann, C.J., "Powder Processing of Synthetic Graphite Flakes", unpublished results.
9. Deepak, A., Dissemination Techniques for Aerosols, A. Deepak Publishing, Virginia(1983).
10. Fuchs, N.A., The Mechanics of Aerosols, Pergamon Press, Macmillam Company, New York(1964).